

# SEGMENTATION OF BRAIN MR IMAGES USING ROUGH SET BASED INTUITIONISTIC FUZZY C-MEANS

GAGAN KODURU<sup>1</sup>, KUDA NAGESWARA RAO<sup>2</sup>, ANUPAMA NAMBURU<sup>3</sup>, SIBI CHAKKARAVARTHY<sup>4</sup>

<sup>1</sup>Part Time Scholar, Andhra University, Department of CS&SE, Visakhapatnam, India

<sup>2</sup>Professor, Andhra University, Department of CS&SE, Visakhapatnam, India

<sup>3</sup>Associate Professor, Vellore Institute of Technology, Department of CSE, Amaravati, India

<sup>4</sup>Associate Professor, Vellore Institute of Technology, Department of CSE, Amaravati, India

E-mail: <sup>1</sup>[gagan.koduru@gmail.com](mailto:gagan.koduru@gmail.com), <sup>2</sup>[knrao2038@gmail.com](mailto:knrao2038@gmail.com), <sup>3</sup>[namburianupama@gmail.com](mailto:namburianupama@gmail.com)

## ABSTRACT

Intuitionistic fuzzy sets and rough sets are widely used for medical image segmentation, and recently combined together to deal with uncertainty and vagueness in medical images. In this paper, a rough set based intuitionistic fuzzy c-means clustering algorithm is proposed for segmentation of the magnetic resonance (MR) brain images. Firstly, we proposed Generalized intuitionistic rough fuzzy c-means [1] algorithm to overcome the dependency with the membership function, parameter tuning and histogram based initial selection of centroids to avoid local minima. In this paper, a modified generalized rough intuitionistic fuzzy c-means is proposed to avoid the histogram-based selection of initial centroids, instead from the obtained intuitionistic regions the centroids are calculated. Also, a minimized distance measure is proposed to improve the performance in all considered scenarios. Experimental results demonstrate the superiority of proposed algorithm.

**Keywords:** *Intuitionistic Fuzzy Sets, Segmentation, Rough Sets, Brain Image, Soft Sets*

## 1. INTRODUCTION

Although there is tremendous improvement in medical image acquisition devices, still the medical images are subject to noise and bias field. These artifacts are the resultant of improper acquisition device or process or the person movements during acquisition of image. These artifacts make the segmentation of medical images more challenging. The magnetic resonance (MR) brain image is often segmented into white matter (WM), gray matter (GM) and cerebro spinal fluid (CSF) and is important to study the functioning of brain, treatment arranging and quantitative examination.

Cluster analysis is a technique for finding natural groups present in the data. It divides a given data set into a set of clusters in such a way that two objects from the same cluster are as similar as possible and the objects from different clusters are as dissimilar as possible. In effect, it tries to mimic the human ability to group similar objects into classes and categories. Clustering techniques have been effectively applied to a wide range of engineering and scientific disciplines such as

pattern recognition, machine learning, psychology, biology, medicine, computer vision, communications, and remote sensing.

Recently, intuitionistic fuzzy sets (IFS) are applied to image segmentation considering the non-membership, hesitancy in conjunction with the membership functions. Atanassov [2] performed the study on theory and application of intuitionistic fuzzy sets. The appliance of intuitionistic fuzzy sets to diagnosing is bestowed within the work [3]. Clustering algorithm is proposed using intuitionistic fuzzy sets with association coefficients for defining the membership functions [4]. The advantage with this theory is that the n-dimensional information  $x_p$  will be portrayed in IFS with a vector of triplet, i.e.,  $(\mu(x_1), \pi(x_1), \gamma(x_1)), (\mu(x_2), \pi(x_2), \gamma(x_2)), \dots, (\mu(x_n), \pi(x_n), \gamma(x_n)))$  rather than a single  $\mu(x)$  as in fuzzy set theory. The illustration of IFS as a vector of triplet having self-doubt membership provides another degree of freedom to manage uncertainty and ambiguity.

There are two main strategies in clustering technique namely crisp and fuzzy clustering technique. Due to various situations, for images,

issues like small scale of spatial resolution, poor illumination, presence of noise, intensity imbrication leads crisp segmentation a hard task. Among numerous clustering techniques, fuzzy c-means algorithm is more significant because of its robustness. Although it is robust it works only on the images without noise. In order to overcome these drawbacks, the image is pre-processed before commencing the clustering process.

Recently, Bezdek [20] defined the concepts of intuitionistic fuzzy similarity degree, intuitionistic fuzzy similarity matrix and intuitionistic fuzzy equivalence matrix, and then gave a procedure for transforming the intuitionistic fuzzy similarity matrix into the intuitionistic fuzzy equivalence matrix. After that, a clustering technique of IFSs was proposed on the basis of the k-cutting matrix of the interval-valued matrix. However, in the above clustering technique, all the given intuitionistic fuzzy information is first transformed into the interval-valued fuzzy information. The intuitionistic fuzzy similarity degrees derived by using distance measures are interval numbers, and both the intuitionistic fuzzy similarity matrix and the intuitionistic fuzzy equivalence matrix are also interval-valued matrices. As a result, this clustering technique requires much computational effort and cannot be extended to cluster IVIFSs, and more importantly, it produces the loss of too much information in the process of calculating intuitionistic fuzzy similarity degrees, which implies a lack of precision in the final results.

Chaira and Tamalika [5, 6] projected novel IFS c-means for edge detection and segmenting medical images with Yager based intuitionistic fuzzy membership degree. Atanassovs intuitionistic fuzzy membership function [7] is recently is used to verify the best threshold for gray-level image segmentation. Ananthi et al. [8], projected grey scale image segmentation using multiple membership functions, interval-valued intuitionistic fuzzy for brain tumor segmentation [9] and a Sugeno fuzzy generator based intuitionistic fuzzy C-means for crop images [10]. Verma [11, 12] used a novel fuzzy technique for considering spatial context and Dubey [13] used complement function for working on brain image segmentation. The IFS based most of the algorithms can handle the noise and INU present within the images. The advantage of using IFS based algorithms is that they efficiently handle the noise and INU present in the brain images. However, the necessity of triple vector membership for defining IFS limits their use. Generalized intuitionistic rough fuzzy c-means [1]

algorithm is proposed to overcome the dependency with the membership function, parameter tuning, and histogram based initial selection of centroids to avoid local minima. However, the initial centroids are computed based on histogram peaks and the window used in calculation is increasing time and the image becomes smooth.

In this paper, we work on centroid calculations and find a way to reduce time required. While doing our research we found out that the time required was way more and it can be handled for better performances. So, we reduce window size and improve performance. In this paper, a modified generalized rough set based intuitionistic fuzzy clustering algorithm is proposed to calculate initial centroids using the image itself and minimize the use of window. The proposed algorithm overcomes the drawback of generalized intuitionistic fuzzy c-means proposed in [1].

The organization of the later paper is as follows: The background of the proposed algorithm for image segmentation is discussed in Section 2. The proposed modified generalized rough intuitionistic fuzzy c-means (MGRIFCM) is presented in Section 3. Implementation and experimental results of the proposed hybrid algorithm is presented in section 4. Conclusions and the future scope of the proposed algorithms are presented in Section 5.

## 2. BACKGROUND

### 2.1 Intuitionistic Fuzzy Sets

The IFS outlined by Atanassov [2] is that the generalized version of fuzzy sets is characterized by a membership, hesitancy and non-membership values. The membership indicates the degree of pixel being part of the cluster, the non-membership indicates the non being part of a cluster and also the hesitancy is indeterminacy of the pixel element being part of the cluster. This definition of hesitancy provides a further information to represent imperfect data in comparison to fuzzy sets. An intuitionistic fuzzy set  $A$  for a finite set  $X$  is expressed as given below.

$$A = \{(x, \mu_A(x), \pi_A(x)) \mid x \in X\} \quad (1)$$

With  $\gamma_A(x) = 1 - (\mu_A(x) + \pi_A(x))$  where the functions  $\mu_A(x)$ ,  $\pi_A(x)$  indicates the degree of membership (being part of cluster) and non-membership (not being part) of an element in finite set  $X$ . The function  $\gamma_A(x)$  is the intuitionistic fuzzy index that indicates the hesitation degree of element. The triple vector defined with the

parameters  $0 \leq \mu A(x), \gamma A(x), \pi A(x) \leq 1$  need to be obtained for every element in the finite set  $X$  in order to be called as intuitionistic fuzzy sets. Hence, every pixel is represented with three membership function that assist in minimizing the noise, bias and accurately assigning the pixel to the cluster.

### 2.2 Rough Set

Rough sets are efficient tools to approximate the uncertainty present in the data with lower and upper approximation. Let  $U$  denote the universe and  $R$  is an equivalence relation and  $U/R$  is a set of  $n$  equivalence classes  $\{x_1, x_2, \dots, x_n\}$  which form partitions in  $X$ . The pair  $(U, R)$  is the approximation space. The lower and upper approximations for a subset  $X \subseteq U$  are denoted by:

$$\underline{R}(x_i) = \bigcup_{x_i \in X} x_i \quad \bar{R}(x_i) = \bigcup_{x_i \cap X \neq \phi} x_i \quad (2)$$

$\underline{R}(x_i)$  indicates the lower approximation space of  $X$  where an object  $x_i$  belongs to  $X$ .  $\bar{R}(x_i)$  indicates the upper approximation space of  $X$  where an object  $x_i$  possibly belongs to  $X$ . The approximation space of  $X$  is classified into three distinct regions.

$$\begin{aligned} \text{positive}(x_i) &= \underline{R}(x_i) \\ \text{boundary}(x_i) &= \bar{R}(x_i) - \underline{R}(x_i) \\ \text{negative}(x_i) &= U - \bar{R}(x_i) \end{aligned} \quad (3)$$

## 3. PROPOSED METHODOLOGY

This section describes the flow of complete algorithm for segmentation of brain MR images using generalized intuitionistic fuzzy set based on rough sets.

### 3.1 Intuitionistic Fuzzy Representation of Image

The intuitionistic fuzzy image representation is used for image segmentation in [6, 11, 13]. The observed image with size  $M * N$  be denoted as  $X = \{x_i/x_i \text{ is the value of the } i^{\text{th}} \text{ pixel in the image}\}$  where  $1 \leq i \leq M * N$ . The image  $X$  is represented in intuitionistic fuzzy set as

$$A = \{(x_i, \mu(x_i), \pi(x_i)) \mid x_i \in X\} \quad (4)$$

With  $\gamma(x_i) = 1 - (\mu(x_i) + \pi(x_i))$  where  $\mu(x_i)$  is the membership value,  $\pi(x_i)$  is the non-membership value and  $\gamma(x_i)$  indicates the hesitation value of  $x_i$  pixel.

### 3.2 Intuitionistic Rough Fuzzy Region Determination

The existing intuitionistic rough fuzzy algorithms [6, 11, 13] used fuzzy generator functions like Yager's complement, Sungeno's complement, Gaussian and combined functions etc., to get the rough regions. The performance of the segmentation depends on the fuzzy membership functions accustomed to generating the intuitionistic set. The generalized intuitionistic fuzzy c-means in [1] proposed a new approach by eliminating the utilization of fuzzy generator functions to outline the IFS. The algorithm used generalized rough sets [14] to determine three rough regions namely deterministic, hesitancy and non-deterministic regions. These regions in turn are used to define intuitionistic fuzzy set. The rough regions are calculated by obtaining threshold based on the distances between each pixel value  $x_i$  and each unique intensity level  $L_k$  present in the image. The distance is calculated using the Eq. 5 given below

$$d_i(k) = \frac{\sqrt{\sum_{k \in NH_i} (x_i - L_k) / |NH_i|}}{L_{max} - L_{min}} \quad (5)$$

Where,  $NH_i$  is the neighborhood of the pixel  $x_i$  and  $|NH_i|$  is the cardinality of the neighborhood.  $k$  is the unique number of intensity levels in the  $NH_i$  and  $L_{max}$  is the maximum intensity,  $L_{min}$  is the minimum intensity. Here, the use of neighborhood makes the algorithm more time complex. In the modified generalized intuitionistic fuzzy c-means the equation is modified to minimize the time complexity and is given in equation 6.

$$d_i(k) = \frac{\sqrt{\sum_i^{M * N} (x_i - L_k)}}{L_{max} - L_{min}} \quad (6)$$

The distance vector obtained with above equation results in  $d_i(k) = \{d_i(L_1), d_i(L_2) \dots, d_i(L_k)\}$  for each pixel  $x_i$ . The maximum distances  $d_{imax}$  and the minimum distances  $d_{imin}$  obtained from these distances are used to estimate two thresholds.

$$\begin{aligned} t_1 &= \frac{1}{M * N} \sum_{i=1}^{M * N} d_{imin} \\ t_2 &= \frac{1}{M * N} \sum_{i=1}^{M * N} d_{imax} \end{aligned} \quad (7)$$

The average minimum distances of the pixels to each cluster is obtained with the  $t_1$  and average maximum distances of the pixels to each cluster is

obtained with  $t_2$ . These thresholds are used to determine the three rough regions namely deterministic  $D(C_j)$ , the hesitancy  $H(C_j)$  and the non-deterministic  $ND(C_j)$  for each cluster  $j$ , the distance  $d_i(C_j)$  between the pixel  $x_i$   $\{i = 1, \dots, M * N\}$  and the mean pixel value  $C_j$  of the cluster  $j$  is obtained using the below equation.

$$d_i(C_j) = \frac{\sqrt{\sum_{k \in NH_i} (x_i - C_j)^2 / |NH_i|}}{L_{max} - L_{min}} \quad (8)$$

Where  $j = 1, \dots, n$  clusters. This equation is modified to minimize the use of neighborhood and improve the time complexity and given as follows.

$$d_i(C_j) = \frac{\sqrt{\sum_i^{M \times N} (x_i - C_j)^2}}{L_{max} - L_{min}} \quad (9)$$

The pixels belong to cluster  $d_i(C_j)$  if the distance of a pixel to a cluster is less than  $t_1$  and are placed in  $D(C_j)$ , does not belong to the cluster i.e.,  $ND(C_j)$  if distance is greater than  $t_2$  and belong to hesitancy  $H(C_j)$  if distance lies between  $t_1$  and  $t_2$ . Hence, thresholds are used to group the pixels into three rough regions.

$$x_i = \begin{cases} D(C_j); & \text{if } d_i(C_j) \leq t_1 \\ H(C_j); & \text{if } t_1 \leq d_i(C_j) \leq t_2 \\ ND(C_j); & \text{otherwise} \end{cases} \quad (10)$$

In order to avoid the use of histogram based optimized centroids the pixels grouped into the three regions are used to compute the centroids to avoid additional computation. The mean value of pixels present in the three regions are considered as new centroids and are computed with the below equations.

$$CD_j = \frac{D(C_j)}{|D(C_j)|}, CH_j = \frac{H(C_j)}{|H(C_j)|}, CND_j = \frac{CND(C_j)}{|CND(C_j)|} \quad (11)$$

Where  $CD_j$ ,  $CH_j$  and  $CND_j$  are new centroids obtained from the regions. Using these regions, the intuitionistic fuzzy set  $\mu(x_i)$ ,  $\pi(x_i)$  and  $\gamma(x_i)$  values are calculated. The membership value  $\mu(x_i)$  is computed using the deterministic region using the below Eq. 12.

$$\mu(x_i) = \frac{1}{\sum_{c=1}^n \left( \frac{\|D(C_j) - CD_j\|}{\|D(C_j) - CD_c\|} \right)^{\frac{2}{m-1}}} \quad (12)$$

Compute the non-membership value  $\pi(x_i)$  with the non-deterministic region and the hesitation value  $\gamma(x_i)$  using the hesitancy region by making use of Equations. (13)-(14).

$$\pi(x_i) = \frac{1}{\sum_{c=1}^n \left( \frac{\|ND(C_j) - CND_j\|}{\|ND(C_j) - CND_c\|} \right)^{\frac{2}{m-1}}} \quad (13)$$

$$\gamma(x_i) = \frac{1}{\sum_{c=1}^n \left( \frac{\|H(C_j) - CH_j\|}{\|H(C_j) - CH_c\|} \right)^{\frac{2}{m-1}}} \quad (14)$$

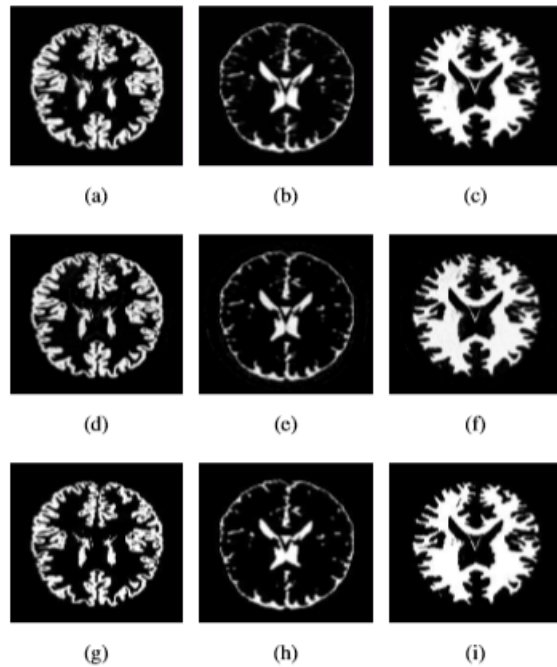


Figure.1. (a)(b)(c) ground truth images of GM, CSF, WM. (d)(e)(f) rough regions for GM, CSF, WM. (g)(h)(i) extracted tissues using MGRIFCM

Table 1 Data sets used for simulation

Dimension	Dataset	Number of Images	Image Size
2D	Brain Web	20	181*217
2D	IBSR	20	256*128

### 3.3 Intuitionistic Fuzzy Clustering

The intuitionistic fuzzy clustering is performed by minimizing objective function  $J$  in the below equation which is obtained by modifying the equation Eq. 15.

$$J = \sum_{i=1}^{M*N} \sum_{j=1}^n (\mu_{IFS}(x_i))^m \|d_{IFS}(x_i, C_j)\|^2 \quad (15)$$

Where  $d_{IFS}(x_i, C_j)$  the total distance of all the pixels to the centroids. In order to handle noise and INU in the MR brain images the Euclidean distance based on intuitionistic fuzzy set [15] with  $\mu(C_j)$  the mean centroid of the pixel  $x_i$ .

$$d_{IFS}(x_i, C_j) = \left\{ \begin{array}{l} \frac{1}{2}((\mu(x_i) - (CD_j))^2 \\ + (\gamma(x_i) - (CH_j))^2 \\ + (\pi(x_i) - (CND_j))^2) \end{array} \right\}^{\frac{1}{2}} \quad (16)$$

Using this intuitionistic fuzzy distance measure, the partition matrix and cluster centroid are updated as

$$\mu_{IFS}(x_i) = \frac{1}{\sum_{c=1}^n \left( \frac{\|d_{IFS}(x_i, C_j)\|}{\|d_{IFS}(x_i, C_c)\|} \right)^{\frac{2}{m-1}}} \quad (17)$$

$$C_j = \frac{\sum_{x_i \in X} (\mu_{IFS}(x_i))^m \mu(x_i)}{\sum_{x_i \in X} (\mu_{IFS}(x_i))^m} \quad (18)$$

The modified generalized rough intuitionistic fuzzy c-means is also iterative and stops when the clusters are stable.

### 3.4 Generalized Rough Intuitionistic Fuzzy c-means Clustering Algorithm (GIRFCM)

The steps in the Generalized intuitionistic rough fuzzy c-means clustering algorithm are listed below.

**Algorithm 1** Algorithm to segment MR brain image using generalized rough intuitionistic fuzzy sets

**INPUT:** 2D MR brain image  $X$ , number of clusters  $n$ ,  $\epsilon$  the value between [0,1] for exit criteria.

**OUTPUT:**  $n$  clusters extracted indicating the regions of brain.

**initialize** the  $\mu_{IFS}(x_i)^l$  to zeros.

**for all**  $L_k$  in  $L$  different intensities **do**

**for all**  $x_i$  in  $X$  **do**

**calculate** the  $d_i(k)$  distance using Eq. 6

**end for**

**end for**

Find the two threshold  $t_1$  and  $t_2$  using Eq. 7.

Find the initial centroids using Eq. 11.

**While 1 do**

**for all**  $j$  in  $n$  clusters **do**

**for all**  $x_i$  in  $X$  **do**

**Calculate** the distance between the pixel  $x_i$  and the centroid  $C_j$  using Eq. 9.

**end for**

**end for**

**for all**  $j$  in  $n$  clusters **do**

**for all**  $x_i$  in  $X$  **do**

            Obtain the three regions and their intuitionistic membership values using Eq. 10-14

**end for**

**end for**

**for all**  $j$  in  $n$  clusters **do**

**for all**  $x_i$  in  $X$  **do**

            Obtain the intuitionistic distance  $d_{IFS}(x_i, C_j)$  using the Eq.16.

**end for**

**end for**

Update the partition matrix  $\mu_{IFS}(x_i)$  and the cluster centroid  $C_j$  using Eq. 17 and Eq. 18.

Find the similarity coefficient( $sc$ ) between  $\mu_{IFS}(x_i)^l$  and  $\mu_{IFS}(x_i)^{l+1}$ .

**if**  $sc \leq \epsilon$  (exit criteria) **then**

**break**

**else**

$\mu_{IFS}(x_i)^l = \mu_{IFS}(x_i)^{l+1}$

**continue**

**end if**

**end while**

**Extract** the  $n$  cluster using the stable  $\mu_{IFS}(x_i)$

## 4. IMPLEMENTATION AND EXPERIMENTAL RESULTS

### 4.1 Experimental Setup

The MGRIFCM algorithm is experimented on brain databases namely: (i) Simulated Brain Web database [16] and (ii) IBSR database [17]. The Brain Web database images are in MINC format, IBSR images are of .hrd or .bit8 format and their image sizes are indicated in **Table 1**.

The software (medical image processing, analysis and visualization) MIPAV[18] is used to



preprocess the image. The algorithm is executed in MATLAB 10.1 on 1.8 GHz Intel core i3 processor.

In the experimental setup for all images to apply proposed segmentation MGRIFCM algorithm, the number of clusters is taken as  $n = 3$  (pertaining to GM, WM, and CSF). The fuzzifier constant is set as  $m = 2$  and the exit criteria is set as 0.01 are used to check the performance of the algorithm.

#### 4.2 Simulated Brain Images

The first experiment is performed on brain web database containing 2D axial view of T1-weighted simulated brain 20 images of slice number 90 with thickness 1 mm, different INU (INU = 0, INU = 20 and INU=40) and noise level (0%, 1%, 3%, 5% ,7% and 9%). **Figure - 2** shows the results of MGRIFCM executed with varied noise levels and varied INU. The visual results proved that the tissue segmentation obtained by applying proposed algorithm is consistent with the ground truth.

**Figure - 3** shows the results of the proposed algorithms compared with other algorithms namely KM [19], FCM [20], RFCM [21], RIFCM [13] and

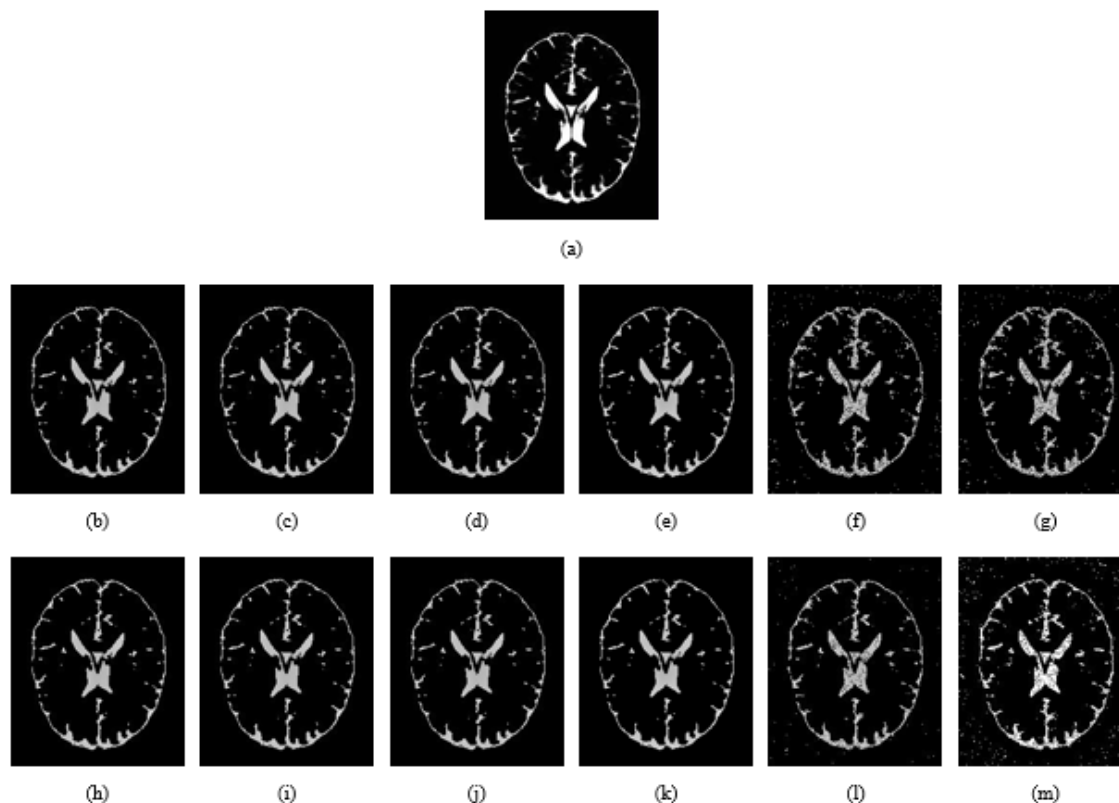
GRIFCM [1] for WM of phantom image with 20% INU and 5% Noise. The proposed segmentation algorithm is further implemented on images with different noise levels. The comparison with other segmentation algorithms demonstrates that the proposed algorithm has the most accurate segmentation and has the most effective ability to segment the tissues in presence of noise and INU.

#### 4.3 Clinical Brain Images

Further, the experiment is performed on IBRS clinical database for 20 slices of MR brain images of ANA1 and ANA2 images. **Figure - 4** shows T1 weighted clinical MR images of slices number 123 before segmentation, and the extracted WM, GM and CSF after segmentation using proposed MGRIFCM.

#### 4.4 Quantitative Analysis

The validation of the segmentation results is performed by quantitative comparison with the ground truth using performance measures namely, *jaccards coefficient (JC)*, *Dice coefficient (DC)* and *segmentation accuracy (SA)*.



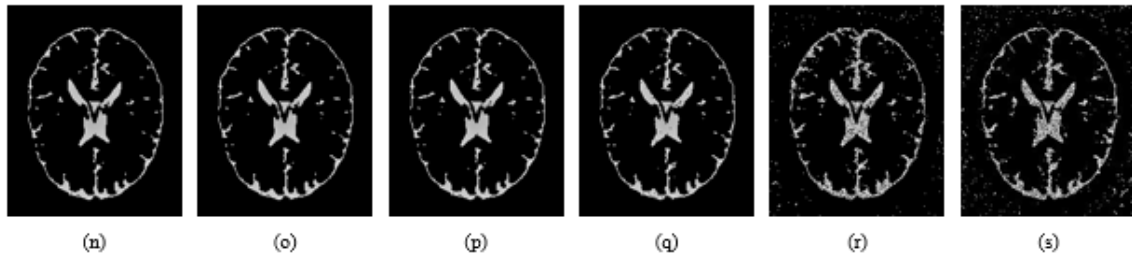


Figure. 2. Segmentation results of proposed algorithm MGRIFCM for T1 weighted Phantom image of 1mm thickness synthetic data. (a)Ground truth of CSF Phantom image column wise. (b)(c)(d)(e)(f)(g) CSF extracted in presence of 0% , 1%, 3%, 5%, 7% and 9% noise with 0% INU. (h)(i)(j)(k)(l)(m) CSF extracted in presence of 0% , 1%, 3%, 5%, 7% and 9% noise with 20% INU.(n)(o)(p)(q)(r)(s) CSF extracted in presence of 0% , 1%, 3%, 5%, 7% and 9% noise with 40% INU.



Figure. 3. Comparison of Algorithms applied to phantom image with 20% INU and 5% Noise. (a) Ground truth of the WM . (b)Extracted using KM. (c) Extracted using FCM. (d) Extracted using RFCM. (e)Extracted using IFCM. (f) Extracted using GRIFCM. (g) Extracted using MGRIFCM .

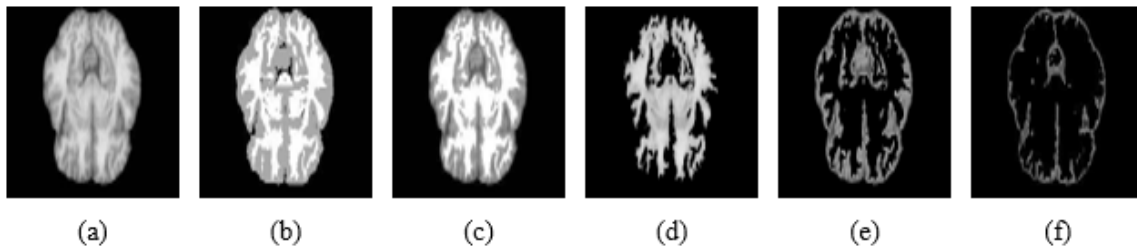


Figure. 4. (A) ANA2 Image Of IBSR Database Slice No 123 Before Segmentation. (B) Ground Truth Of ANA2 Image Slice No 123. (C) Segmentation Result Of ANA2 Image Slice No 123 Using MGRIFCM.(D, E, F) Extracted WM, GM And CSF Using MGRIFCM.

Table 2. Comparative Performance (*Dice Coefficient*) Of Proposed Algorithms On Simulated Brain Images With Different Noise Levels And INU For GM, CSF, WM Of Phantom Image

Intensity non-uniformity	Tissue type	0% Noise	1% Noise	3% Noise	5% Noise	7% Noise	9% Noise
0% INU	GM	0.9834	0.9648	0.9418	0.9164	0.9082	0.8804
	CSF	0.9612	0.9561	0.9482	0.9252	0.9186	0.8968
	WM	0.9842	0.9872	0.9760	0.9664	0.9462	0.9108
20% INU	GM	0.9572	0.9563	0.9280	0.8854	0.8396	0.8012
	CSF	0.9564	0.9542	0.9464	0.9266	0.8742	0.8556
	WM	0.9861	0.9768	0.9754	0.9652	0.9428	0.8990
40% INU	GM	0.9243	0.9262	0.9024	0.8732	0.8288	0.7856
	CSF	0.9471	0.9458	0.9380	0.9198	0.8778	0.8571
	WM	0.9681	0.9693	0.9662	0.9486	0.9268	0.8974

**Table 3.** Comparative Performance (Segmentation Accuracy) Of Proposed Algorithms On Simulated Brain Images With Different Noise Levels And INU For GM, CSF, WM Of Phantom Image

Intensity non-uniformity	Tissue type	0% Noise	1% Noise	3% Noise	5% Noise	7% Noise	9% Noise
0% INU	GM	0.9888	0.9862	0.9745	0.9652	0.9456	0.9368
	CSF	0.9954	0.9928	0.9898	0.9874	0.9762	0.9586
	WM	0.9942	0.9914	0.9883	0.9798	0.9666	0.9472
20% INU	GM	0.9836	0.9822	0.9743	0.9654	0.9478	0.9368
	CSF	0.9988	0.9924	0.9873	0.9864	0.9786	0.9649
	WM	0.9962	0.9861	0.9852	0.9779	0.9689	0.9590
40% INU	GM	0.9702	0.9711	0.9649	0.9446	0.9256	0.9162
	CSF	0.9946	0.9935	0.9914	0.9887	0.9784	0.9653
	WM	0.9812	0.9841	0.9816	0.9724	0.9632	0.9437

**Table 4.** Comparative Performance (Jaccards Coefficient) Of Different Segmentation Algorithms On Phantom Brain Image With 0% INU And Varying Noise Level.

Gaussian Noise	Tissue type	KM Tou's	RKM Lingras's	FCM Chuang's	RFCM Lingras's	GFCM Ji's	SFRFCM Gagan's	RIFCM Dubey's	GRIFCM Gagan's	MGRIFCM Proposed
0%	GM	0.9542	0.9652	0.9522	0.9658	0.9530	0.9752	0.9703	0.9812	0.9822
	CSF	0.9720	0.9743	0.9728	0.9782	0.9679	0.9264	0.8992	0.9126	0.9091
	WM	0.9580	0.9605	0.9636	0.9702	0.9620	0.9626	0.9564	0.9689	0.9685
3%	GM	0.8423	0.8562	0.8540	0.8610	0.8682	0.8902	0.9565	0.9681	0.9685
	CSF	0.8202	0.8572	0.8460	0.8624	0.8484	0.8912	0.9116	0.9281	0.9199
	WM	0.8242	0.8656	0.8426	0.8718	0.8855	0.9164	0.9456	0.9623	0.9622
9%	GM	0.7141	0.7853	0.7248	0.7756	0.6820	0.7958	0.9257	0.9503	0.9511
	CSF	0.6239	0.7832	0.7698	0.7806	0.7622	0.7786	0.9016	0.9189	0.9098
	WM	0.6242	0.6304	0.7686	0.7492	0.7854	0.7842	0.9193	0.9254	0.932

**Table 5.** Comparison Of Iterations Required For Execution By Different Segmentation Algorithms Initialization

	KM	RKM	FCM	RFCM	GRFCM	SFRFCM	RIFCM	GRIFCM	MGRIFCM
Histogram	10	9	31	29	19	18	20	18	18
Random	43	40	65	54	22	45	-	20	20

The JC between two data sets is the result of division between the number of properties that are common to both data sets divided by the number of properties.

$$Jaccard\ coefficient = \frac{A \cap B}{A \cup B} \quad (19)$$

Where A is the resultant segmented image, B is the ground truth image. If the Jaccard coefficient is above 70%, it means that the segmentation result is good. The DC between two data sets is the result of division between the twice the number of properties

that are common to both data sets divided by the number of properties present in A and B.

$$Dice\ coefficient = \frac{2 | A \cap B |}{| A | + | B |} \quad (20)$$

Where A is the resultant segmented image, B is the ground truth image. Segmentation accuracy(SA) is another measure which is mostly used to compare the similarities between the segmented result and the ground truth image. In order to calculate Segmentation accuracy, for each segmentation result four parameters are calculated.



1. True positive (TP): Number of true pixels in the ground truth correctly detected as segmented pixels.
2. True negative (TN): Number of false pixels in the ground truth correctly identified as segmented pixels.
3. False positive (FP): The numbers of true pixels in the ground truth are not found in the segmented region.
4. False negative (FN): The number of false pixels in the ground truth which are not present in the segmented region.

$$\text{Segmentation Accuracy} = \frac{TP + FN}{TP + FN + TN + FP} \quad (21)$$

The comparative *jaccards coefficient* results of the KM, RKM, FCM, RFCM, GRFCM, SRFCM, RIFCM and the proposed method MGRIFCM is presented in **Table 4** and the number of iterations required to execute is presented in **Table 5**. The results show that the proposed algorithm outperforms the existing method in considered scenarios. The KM algorithms is simple and executes fast but cannot handle the pixels present in the boundary region. The FCM algorithm can overlap the clusters for better performance but the segmentation result is degraded with the effect of noise. The RKM and RFCM can effectively handle the pixels in the boundary region by reducing the clustering mistakes, hence, improve the segmentation results. However, these methods are affected by the parameter tuning and complex calculations involved in the algorithm. SRFCM produces good results in absence of noise and reduces the complexity in the calculations and free from parameter tuning. However, this method is not performing well in presence of noise. The RIFCM proposed by Dubey uses intuitionistic fuzzy sets to segment the brain images. But this method is dependent on the fuzzy generator functions to determine the three membership functions.

The proposed method is compared to KM, FCM, RFCM, GRFCM and RIFCM with their dice coefficients and the *jaccards coefficients* in table 4. With the comparisons of these algorithms, the proposed method performs very well with highest coefficients values. The proposed method automatically calculates thresholds and based on the thresholds the rough regions are obtained using these regions. Then the membership values of the deterministic, non-deterministic and the hesitancy

of the pixels are calculated. Hence, the proposed method eliminates the drawbacks of dependencies of fuzzy generators and the parameter tuning. Due to these advantages, MGRIFCM proved to be better algorithm for segmenting MR brain images in presence of noise and INU.

Following conclusions can be drawn from the results reported in this paper:

1. It is observed that MGRIFCM is superior to other c-means fuzzy algorithms. Also, MGRIFCM requires lesser time compared to FCM/PCM. Also, the performance of MGRIFCM is significantly higher than other c-means.

2. Use of rough sets and fuzzy memberships adds a small computational load to MGRIFCM algorithm.

3. The indices such as dice, jaccard based on the theory of rough sets provide good quantitative measures for rough-fuzzy clustering. The values of these indices reflect the quality of clustering.

## 5. CONCLUSION

Histogram based centroid approach is good but it is initialized randomly and after histogram calculation. This leads to increase in time to reach the optimal solution. In order to accelerate the segmentation process, region based centroid segmentation is used. In this paper, modified generalized rough intuitionistic fuzzy c-means algorithm has been presented for brain MR medical image segmentation. The algorithms avoid the use of histogram based optimized centroids and instead used the regions generated by generalized rough intuitionistic fuzzy c-means to obtain the centroids. Also, the algorithm minimizes the use of window and neighborhood effect of the pixel as the IFS itself can effectively handle the noise and works well for segmenting brain image segmentation. The algorithm produces accurate results as it is robust to noise, INU and initialization of centroids.

The performance of the proposed algorithms is evaluated on both synthetic and clinical data and hence, the proposed method MGRIFCM produces accurate brain image segmentation when analyzed with the considered performance measures.

## 6. CONFLICT OF INTEREST STATEMENT

The author has no conflict of interest regarding the financial or personal aspect in any manner in regard to this paper.

## REFERENCES

- [1] I Namburu, A., Samayamantula, S. K., and Edara, S. R.: “Generalised rough intuitionistic fuzzy c-means for magnetic resonance brain image segmentation”, IET Image Processing, 2017, 11, (9), pp. 777–785.
- [2] 2 Atanassov, K. T.: “Intuitionistic fuzzy sets”, Fuzzy sets. Syst, 1986, 20, (1), pp. 87–96.
- [3] De, S. K., Biswas, R., and Roy, A. R.: “An application of intuitionistic fuzzy sets in medical diagnosis”, Fuzzy sets. Syst, 2001, 117, (2), pp. 209–213.
- [4] Xu, Z., Chen, J., and Wu, J.: “Clustering algorithm for intuitionistic fuzzy sets”, Inform. Sciences, 2008, 178, (19), pp. 3775–3790.
- [5] Chaira, T.: “A novel intuitionistic fuzzy C means clustering algorithm and its application to medical images”, Appl. Soft Comput., 2011, 11, (2), pp. 1711–1717.
- [6] Chaira, T.: “A rank ordered filter for medical image edge enhancement and detection using intuitionistic fuzzy set”, Appl. Soft Comput., 2012, 12, (4), pp. 1259–1266.
- [7] Melo-Pinto, P., Couto, P., Bustince, H., Barrenechea, E., Pagola, M., and Fernandez, J.: “Image segmentation using Atanassovs intuitionistic fuzzy sets”, Expert Syst. Appl., 2013, 40, (1), pp. 15–26.
- [8] Ananthi, V., Balasubramaniam, P, and Lim, C. P.: “Segmentation of gray scale image based on intuitionistic fuzzy sets constructed from several membership functions”, Pattern Recognit., 2014, 47, (12), pp. 3870–3880.
- [9] Ananthi, V., Balasubramaniam, P, and Kalaiselvi, T: “A new fuzzy clustering algorithm for the segmentation of brain tumor”, Soft Comput., 2016, 20, (12), pp. 4859–4879.
- [10] Balasubramaniam, P and Ananthi, V.: “Segmentation of nutrient deficiency in incomplete crop images using intuitionistic fuzzy C-means clustering algorithm”, Nonlinear Dynam., 2016, 83, (1-2), pp. 849–866.
- [11] Verma, H., Agrawal, R., and Sharan, A.: “An improved intuitionistic fuzzy c-means clustering algorithm incorporating local information for brain image segmentation”, Appl. Soft Comput., 2015, 46, 543–557.
- [12] Verma, H. and Agrawal, R.: “Possibilistic Intuitionistic Fuzzy c-Means Clustering Algorithm for MRI Brain Image Segmentation”, Int. J. Artif. Intell. Tools, 2015, 24, (05), pp. 1550016– 1–1550016–24.
- [13] Dubey, Y. K., Mushrif, M. M., and Mitra, K.: “Segmentation of brain MR images using rough set based intuitionistic fuzzy clustering”, Biocybern. Biomed. Eng., 2016, 36, (2), pp. 413– 426.
- [14] Ji, Z., Sun, Q., Xia, Y., Chen, Q., Xia, D., and Feng, D.: “Generalized rough fuzzy c-means algorithm for brain MR image segmentation”, Comput. Med. Imaging Graph., 2012, 108, (2), pp. 644–655.
- [15] Szmidt, E.: Distances and similarities in intuitionistic fuzzy sets (Springer, 1st edn.).
- [16] Web, B.: “Simulated brain database”, McConnell Brain Imaging Centre, Montreal Neurological Institute, McGill, <http://brainweb.bic.mni.mcgill.ca/brainweb>, 2004.
- [17] “IBSR, The Internet Brain Segmentation Repository”, <http://www.cma.mgh.harvard.edu/ibsr/>.
- [18] McAuliffe, M: “Medical image processing, analysis, and visualization (MIPAV)”, National Institutes of Health, 2009, 4, (0).
- [19] Tou, J. T. and Gonzalez, R. C.: “Pattern recognition”, Reading, Addison-Wesley, MA, 1974.
- [20] Bezdek, J. C., Ehrlich, R., and Full, W.: “FCM: The fuzzy c-means clustering algorithm”, Comput. Geosci., 1984, 10, (2-3), pp. 191–203.
- [21] Maji, P. and Pal, S. K.: “RFCM: a hybrid clustering algorithm using rough and fuzzy sets”, Fund. Inform., 2007, 80, (4), pp. 475–496.